JOURNAL OF AGRICULTURAL AND FOOD CHEMISTRY

Article

pubs.acs.org/JAFC

Structural Changes of High-Amylose Rice Starch Residues following in Vitro and in Vivo Digestion

Jianmin Man,[†] Yang Yang,[†] Changquan Zhang,[†] Xinghua Zhou,[‡] Ying Dong,[‡] Fengmin Zhang,[§] Qiaoquan Liu,*[,†] and Cunxu Wei*[,†]

[†]Key Laboratories of Crop Genetics and Physiology of the Jiangsu Province and Plant Functional Genomics of the Ministry of Education, Yangzhou University, Yangzhou 225009, China

[‡]School of Food and Biological Engineering, Jiangsu University, Zhenjiang 212013, China

[§]Testing Center, Yangzhou University, Yangzhou 225009, China

ABSTRACT: High-amylose cereal starch has a great benefit on human health through its resistant starch content. In this paper, starches were isolated from mature grains of high-amylose transgenic rice line (TRS) and its wild-type rice cultivar Te-qing (TQ) and digested in vitro and in vivo. The structural changes of digestive starch residues were characterized using DSC, XRD, ^{13}C CP/MAS NMR, and ATR-FTIR. TQ starch was very susceptible to digestion; its residues following in vitro and in vivo digestion showed similar structural characteristics with TQ control starch, which suggested that both amorphous and crystalline structures were simultaneously digested. Both amorphous and the long-range order structures were also simultaneously hydrolyzed in TRS starch, but the short-range order (double helix) structure in the external region of TRS starch granule increased with increasing digestion time. The A-type polymorph of TRS C-type starch was hydrolyzed more rapidly than the B-type polymorph. These results suggested that B-type crystallinity and short-range order structure in the external region of starch granule made TRS starch resistant to digestion.

KEYWORDS: *rice, high-amylose starch, structural property, in vitro digestion, in vivo digestion*

INTRODUCTION

Cereal storage starch is a major source of nourishment for humans. For nutritional purposes, starch is classified into three types: rapidly digestible starch, slowly digestible starch, and resistant starch (RS).[1] RS is a portion of starch that cannot be hydrolyzed in the upper gastrointestinal tract and functions as a substrate for bacterial fermentation in the large intestine.[1] RS has been reported to provide many health benefits for humans; for example, RS-enriched food can lower the glycemic and insulin responses and reduce the risk for developing type II diabetes, obesity, and cardiovascular disease.[2] In general, RS content of granular starch is positively correlated with the level of amylose.[3] Therefore, high-amylose cereal crops are attracting considerable attention because of their potential health benefits, along with their industrial uses.[4] Many high-amylose cereal crop varieties have been developed via mutation or transgenic breeding approaches.[5−7]

Starch branching enzymes (SBEs) are responsible for the production of the α-1,6-glucosidic linkages in amylopectin. Three classes of SBEs (SBE I, SBE IIa, and SBE IIb) are known in cereal crops. In maize endosperm, lesion in the SBE IIb gene results in the *amylose extender* (*ae*) phenotype with amylose contents from 50 to 80%.[5] In wheat endosperm, it has been demonstrated that suppression of the expression of SBE IIa is required to yield a very high amylose content (>70%).[6] In barley endosperm, the amylose content increase is very dramatic when both SBE IIa and SBE IIb are reduced, with amylose contents of 65.8 and 89.3% for SBE IIa^{-1}/SBE IIb↓ and SBE IIa^{-1}/SBE IIb^{-1} lines, respectively.[7] In rice endosperm, elimination of SBE I activity does not result in measurable differences in amylose content;[8] mutations eliminating the expression of SBE IIb lead to increased amylose content.[9] Many high-amylose cereal crops with suppression or mutation of SBEs have been proven to contain a high level of RS and show potential health benefits. For example, high-amylose wheat and barley grains have significant potential to improve health by reduction of plasma cholesterol and production of increased large-bowel short-chain fat acids.[6,10]

Rice has the highest starch content among cereal crops and is the staple food of over half the world's population, but its RS content is relatively low. Although high-amylose rices have been developed,[9,11,12] their amylose contents are not very high compared with high-amylose maize, wheat, and barley.[5−7] A high-amylose transgenic rice line (TRS) has been developed by antisense RNA inhibition of both SBE I and SBE IIb in our laboratory, which yields a starch with an amylose content of about 60%.[13,14] TRS starch is identified as having C-type crystallinity, which has a high resistance to HCl hydrolysis, *Bacillus licheniformis* α-amylase hydrolysis, and heating.[13,15] TRS grains are rich in RS,[14] are as safe as the conventional nontransgenic rice for rat consumption,[16] and have shown significant potential to improve the health of the large bowel in rats.[14]

In most mammals, starch digestion and glucose absorption occur mostly in the small intestine. In the intestinal lumen,

Received: July 10, 2012
Revised: August 18, 2012
Accepted: August 23, 2012
Published: August 23, 2012

starch is hydrolyzed by pancreatic α-amylase to maltose and larger oligosaccharides, which are further hydrolyzed to glucose by maltase-glucoamylase and sucrase-isomaltase on the brush-border surface before being absorbed.[17] Most human and animal studies of starch in vivo digestion have been carried out using the digesta collected from the terminal ileum or feces.[18,19] These digesta show the structure of RS that is not digested in the small intestine. Many studies of starch in vitro digestion have also been designed to simulate and investigate digestion in the small intestine.[1,19−21] These in vitro digestion methods provide practical and reproducible approaches to study starch digestibility and its relationship with starch molecular structure. McCleary et al.[22] developed a method for the measurement of RS, in which samples are incubated in a shaking water bath with pancreatic α-amylase (10 mg/mL) and amyloglucosidase (3 U/mL) in sodium maleate buffer (100 mM, pH 6.0) at 37 °C. The procedure reflects in vivo conditions and yields values that are physiologically significant.

In this paper, starches were isolated from mature grains of high-amylose rice TRS and its wild-type rice cultivar Te-qing (TQ) and digested in vitro and in vivo. Structural changes of starch residues at different digestion stages were characterized using differential scanning calorimetry (DSC), X-ray powder diffraction (XRD), solid state ^{13}C cross-polarization magic-angle spinning nuclear magnetic resonance (^{13}C CP/MAS NMR) spectroscopy, and attenuated total reflectance−Fourier transform infrared (ATR-FTIR) spectroscopy. The objective of this study was to obtain a better understanding of the resistance of high-amylose TRS starch to digestion.

MATERIALS AND METHODS

Plant Materials. An *indica* rice cultivar Te-qing (TQ) and its transgenic line (TRS) with high amylose and RS contents were used in this study. TRS was generated from TQ after transgenic inhibition of both SBE I and SBE IIb through an antisense RNA technique and was homozygous for the transgene. The expressions of SBE I and SBE IIb were completely inhibited in TRS grains.[14] TQ and TRS were cultivated in the transgenic close experiment field of Yangzhou University, Yangzhou, China, in 2011, and mature grains were used to isolate starches.

Isolation of Native Starches. Native starches were isolated from mature grains as previously described.[13]

In Vitro Digestive Starch Residue Preparation. The preparation of in vitro digestive starch was carried out according to an AOAC method,[22] using the Megazyme Resistant Starch Assay Kit with a slight modification. One gram of starch sample was digested with 40 mL of pancreatic α-amylase (10 mg/mL) containing amyloglucosidase (3 U/mL) at 37 °C with continuous shaking (100 rpm) in a constant-temperature shaking water bath for different times. Undigested starch residues were obtained by centrifugation (3000*g*, 10 min), subsequently washed three times with ddH_2O and twice with anhydrous ethanol and then dried at 40 °C for 2 days. Control starch without enzyme but subjected to the above experimental conditions was run concurrently. The dried starch residues were ground into powders in a mortar with pestle and passed through a 100-mesh sieve for structural analyses.

In Vivo Digestive Starch Residue Preparation. All animal experiments (including rice diet preparation and Sprague−Dawley rat feeding) were performed according to the method of Zhou et al.[16] The rats in TQ and TRS diet groups were respectively given a diet containing 70% TQ and TRS flours. The nutritional compositions of diets for rats in TQ and TRS diet groups were essentially the same. The stomach, jejunum, and ileum were removed under anesthetia. The digesta were collected from the stomach, jejunum, and ileum by squeeze expulsion and then fixed in anhydrous ethanol at 4 °C prior to analysis. Fresh feces were fixed in anhydrous ethanol. Starches were isolated from the diet, digesta, and feces. Briefly, the diet, digesta, and feces were homogenized with anhydrous ethanol in a mortar with a pestle. The homogenate was filtered with 100-, 200-, 300-, and 400-mesh sieves and centrifuged at 3000*g* for 10 min. The gel-like layer on top of the packed white starch pellet was carefully scraped off and discarded. The precipitated starch was washed six times with SDS wash buffer (62.5 mM Tris-HCl, pH 6.8; 10 mM DTT; 10 mM EDTA; 4% SDS) to remove protein at room temperature. The samples were subsequently washed with ddH_2O, anhydrous ethanol, methanol, and ether twice to remove lipid. Finally, the samples was again washed twice with anhydrous ethanol and then dried at 40 °C for 2 days. The dried starch residues were ground into powders and passed through a 100-mesh sieve for analyses.

Light Microscope Observation. Starch residues of in vivo digesta were stained with iodine as previously described[23] and were observed under the Olympus BX53 light microscope equipped with a CCD camera.

Amylose Content Measurement. The amylose content of starch was determined using the iodine adsorption method of Konik-Rose et al.[24] with some modifications. Ten milligrams of starch was weighed (accurate to 0.1 mg) into a 10 mL screw-capped tube. For defatting, 5 mL of 85% (v/v) methanol was added and incubated at 65 °C for 1 h with occasional vortexing. After centrifugation at 13000*g* for 5 min, the supernatant was removed. The defatting step was then repeated. The starch was dried at 37 °C overnight and then dissolved in 5 mL of urea dimethyl sulfoxide (UDMSO) solution (9 parts DMSO and 1 part 6 M urea). Dissolution was obtained by incubating the mixture at 95 °C for 1 h with intermittent vortexing. A 1 mL aliquot of the starch−UDMSO solution was treated with 1 mL of iodine solution (0.2% I_2 and 2% KI, w/v) and made up to 50 mL with water. The solution was immediately mixed and placed in darkness for 20 min. Apparent amylose content was evaluated from absorbance at 620 nm. The recorded values were converted to percent of amylose by reference to a standard curve prepared with amylose from potato (Sigma-Aldrich A-0512) and amylopectin from corn (Sigma-Aldrich 10120).

DSC Analysis. A DSC (200-F3, Netzsch, Germany) was used to examine the thermal property of starch as described previously.[15]

XRD Analysis. XRD analysis of starch was carried out on an XRD (D8, Bruker, Germany), and the relative crystallinity (%) was measured following the method described by Wei et al.[25]

Solid-State ^{13}C CP/MAS NMR Analysis and Peak-Fitting Procedure. High-resolution solid-state ^{13}C CP/MAS NMR analysis of starch was carried out at B_0 = 9.4T on a Bruker AVANCE III 400 WB spectrometer as described previously.[25] Amorphous starch was prepared by gelatinizing native starch following the method of Wei et al.[25] The ^{13}C CP/MAS NMR spectra were peak fitted by using PeakFit version 4.12. The relative crystallinity was calculated as the proportion of the fitting peak areas of the triplet or doublet relative to the total area of the spectrum at C1 region according to the method described by Paris et al.[26] The quantitative analyses of double-helix, single-helix, and amorphous conformational features within starch were carried out according to the method described by Tan et al.[27] The analysis of the NMR spectra involved the decomposition of the spectra into amorphous and ordered subspectra. The spectrum of amorphous starch was matched to the intensity of control and digestive starches at 84 ppm and was subtracted to produce the ordered subspectrum. The areas of the amorphous and ordered subspectra relative to the total area of the spectrum at C1 region yielded the percentage of amorphous and ordered components, respectively. The computer peak fitting of ordered subspectrum at C1 region yielded four individual peaks at about 99.6, 100.7, 101.4, and 102.6 ppm. The peak at 102.6 ppm was coincident with the C1 chemical shifts of the single-helical V-type conformation, and the peaks at 99.6, 100.7, and 101.4 ppm were double-helix components. By comparison of the areas of single-helix and double-helix peaks at C1 region in the ordered subspectrum, the relative proportions of single-helical and double-helical features within the starches were obtained.[27]

ATR-FTIR Analysis. ATR-FTIR analysis of starch was carried out on a Varian 7000 FTIR spectrometer with a DTGS detector equipped with a ATR single-reflectance cell containing a germanium crystal (45°

Table 1. Amylose Contents, Thermal Properties, and Relative Crystallinities of in Vitro Digestive Starch Residues[a]

		DSC[b]				
starch residue	amylose content[c] (%)	T_o (°C)	T_p (°C)	T_c (°C)	ΔH (J/g)	relative crystallinity[d] (%)
TQ						
0 h	26.5 ± 0.3 a	63.5 ± 0.4 a	74.4 ± 0.1 a	81.2 ± 0.6 ab	13.2 ± 0.5 ab	27.3 ± 0.4 ab
1 h	29.1 ± 0.5 b	66.9 ± 0.5 b	74.6 ± 0.0 a	80.3 ± 0.1 b	13.0 ± 0.2 ab	27.5 ± 0.2 a
2 h	28.7 ± 0.8 b	68.4 ± 0.3 b	75.2 ± 0.1 b	81.2 ± 0.2 bc	14.7 ± 0.5 ab	26.5 ± 0.1 b
4 h	29.0 ± 1.2 b	68.4 ± 0.1 b	74.8 ± 0.2 ab	80.7 ± 0.1 b	13.4 ± 0.1 a	29.2 ± 0.5 c
8 h	29.6 ± 0.2 b	71.5 ± 0.1 c	77.0 ± 0.0 c	82.9 ± 0.4 ac	14.1 ± 0.2 b	30.4 ± 0.8 c
TRS						
0 h	63.5 ± 0.5 a	67.0 ± 0.3 a	76.9 ± 0.1 a	87.4 ± 0.7 ab	7.8 ± 0.7 a	17.5 ± 0.4 a
1 h	55.6 ± 0.8 b	69.1 ± 0.0 b	76.3 ± 0.4 ab	85.3 ± 0.0 a	6.9 ± 0.3 a	17.1 ± 0.3 ab
2 h	53.9 ± 0.9 c	68.6 ± 0.2 bc	76.2 ± 0.3 acd	85.8 ± 0.4 ab	7.2 ± 0.5 a	16.9 ± 0.3 ab
4 h	50.9 ± 0.4 d	69.2 ± 0.3 bd	76.4 ± 0.1 bc	85.5 ± 0.1 ab	6.9 ± 0.2 a	16.3 ± 0.3 bc
8 h	49.1 ± 0.4 e	69.3 ± 0.0 cd	77.0 ± 0.1 ad	86.0 ± 0.3 ab	6.1 ± 0.1 a	15.6 ± 0.2 c
16 h	46.8 ± 0.5 f	70.1 ± 0.3 bd	77.6 ± 0.0 b	86.3 ± 0.2 b	4.2 ± 0.3 b	16.2 ± 0.2 c

[a]Data (mean ± SD) in the same column with different letters are significantly different ($p < 0.05$). [b]T_o, onset temperature; T_p, peak temperature; T_c, conclusion temperature; ΔH, enthalpy of gelatinization. [c]The amylose content was determined by the iodine adsorption method.[24] [d]The relative crystallinity was obtained from XRD.[25]

incidence angle) (PIKE Technologies, USA) as previously described.[25] Spectra were corrected by a baseline in the region from 1200 to 800 cm^{-1} before deconvolution was applied using Resolutions Pro. The assumed line shape was Lorentzian with a half-width of 19 cm^{-1} and a resolution enhancement factor of 1.9. Intensity measurements at 1047, 1022, and 995 cm^{-1} were performed on the deconvoluted spectra by recording the height of the absorbance bands from the baseline using Adobe Photoshop 7.0 image software.

Statistical Analysis. The amylose content determination was replicated three times, DSC analysis was replicated twice, and spectra of XRD, ^{13}C CP/MAS NMR, and ATR-FTIR were quantitatively analyzed with relative software at least twice. Mean values and standard deviation values were reported. Analysis of variance (ANOVA) by Tukey's test ($p < 0.05$) was evaluated using the SPSS 16.0 Statistical Software Program.

RESULTS AND DISCUSSION

In Vitro Digestibilities of Starches. Compared with TQ starch, the amylose content of TRS starch is dramatically increased from 22.5 to 55.4% in milled rice flour[28] and from 27.2 to 64.8% in isolated starch.[14] A positive correlation is evident between RS and amylose content. In grains of TRS, the RS content is 14.6% measured according to the AOAC method, whereas little or no RS is detected in TQ grain.[14] When the Englyst assay method is used, the RS content is significantly increased from 18.3% in TQ flour to 33.4% in TRS flour and from 33.3% in TQ starch to 55.3% in TRS starch.[28] TRS starch has a higher resistance to *B. licheniformis* α-amylase hydrolysis than TQ starch.[13] In this study, starches were simultaneously digested in vitro by pancreatic α-amylase and amyloglucosidase, and the residual quantities of digestive starches were significantly lower in TQ than in TRS, especially after 4 h of digestion (data not shown). TQ starch was almost completely hydrolyzed for 16 h of digestion, and no residue was obtained for analyzing its structural property.

Amylose Contents of in Vitro Digestive Starch Residues. Amylose contents of in vitro digestive starch residues are presented in Table 1. The amylose content plays an important role in the starch internal quality and its property. In starch granule, some amylose forms the double helices, some amylose and lipid form a amylose−lipid complex, and the other amylose is located in the starch amorphous region. The double helices associate to form crystallinity, which resist enzyme hydrolysis. The amylose−lipid complex has high resistance to amylase hydrolysis.[29] Amylose contents in TQ starch residues did not show significant change during in vitro digestion, but that of TRS starch residues rapidly decreased at initial digestion (1 h) and then gradually decreased with increasing digestion time. Amylose is mainly distributed in the central hilum of TQ starch.[23] The similar amylose contents of digestive TQ starch residues suggested that amylose and amylopectin were simultaneously hydrolyzed by pancreatic α-amylase and amyloglucosidase. Amylose is mainly distributed in the central hilum and surrounding region of the TRS starch granule.[23] The amylose content of TRS starch residues decreased during in vitro digestion, which might result from the easy degradation of amylose in the surrounding region of the TRS starch granule.

Thermal Properties of in Vitro Digestive Starch Residues. The thermal properties of in vitro digestive starch residues measured by DSC are listed in Table 1. The value of onset temperature in TQ digestive starch residues was significantly higher than that in TQ control starch, but the values of peak temperature, conclusion temperature, and gelatinization enthalpy in TQ digestive starch residues were similar to that in TQ control starch. The values of gelatinization temperature in TRS digestive starch residues were similar to that in TRS control starch, but the value of gelatinization enthalpy in TRS digestive starch residue was lower than that in TRS control starch.

Gelatinization involves the uncoiling and melting of the external chains of amylopectin that are packed together as a double helix in clusters. Gelatinization temperature was influenced by the molecular architecture of the crystalline region, which corresponds to the distribution of amylopectin short chains, and not by the proportions of crystalline regions, which corresponds to the amylose/amylopectin ratio. The difference in gelatinization temperature may be attributed to the difference in amylose content, size, form, and distribution of starch granules, as well as to the internal arrangement of starch fractions within the granule.[30] Gelatinization enthalpy is due mainly to the disruption of the double helices rather than the long-range disruption of crystallinity.[31] Compared with undigested starch, waxy maize starch residues following in vitro pancreatic α-amylase and amyloglucosidase hydrolysis show an increase in onset temperature and similar enthalpy.

The increase in the relative number of smaller granules after enzyme hydrolysis causes an increase in the onset temperature. Similar enthalpy shows simultaneous hydrolysis of both crystalline and amorphous regions of waxy maize starch by in vitro digestion.[30] In this study, the thermal properties of in vitro digestive TQ starch residues were in agreement with those of waxy maize starch. TRS and TQ starches show different morphological structure,[23] crystallinity,[13] and hydrolysis properties,[13] which resulted in the different thermal properties of in vitro digestive TQ and TRS starch residues.

XRD Spectra of in Vitro Digestive Starch Residues. The XRD patterns of TQ and TRS starch residues from in vitro digestion treatment are presented in Figure 1, and their relative crystallinities are listed in Table 1. To exclude the effect of enzyme solution on the structural properties, we used control starch instead of native starch. Starches can be classified to A-, B-, and C-type crystallinity by XRD spectra. A-type starch has strong diffraction peaks at about 15° and 23° 2θ and an unresolved doublet at around 17° and 18° 2θ. B-type starch gives the strongest diffraction peak at around 17° 2θ, a few small peaks at around 15°, 20°, 22°, and 24° 2θ, and a characteristic peak at about 5.6° 2θ. C-type starch is a mixture of both A- and B-type polymorphs and can be further classified in to C_A-type (closer to A-type), C-type, and C_B-type (closer to B-type) according to the proportion of A-type and B-type polymorphs. The typical C-type starch shows strong diffraction peaks at about 17° and 23° 2θ and a few small peaks at around 5.6° and 15° 2θ. The XRD patterns of C_A- and C_B-type starches show some slight differences from that of typical C-type. C_A-type starch shows a shoulder peak at about 18° 2θ and strong peaks at about 15° and 23° 2θ, which are indicative of the A-type polymorph. C_B-type starch shows two shoulder peaks at about 22° and 24° 2θ and a weak peak at about 15° 2θ, which are indicative of the B-type polymorph. The peak at 20° 2θ is the amylose−lipid complex diffraction peak. The peak at 15° 2θ in A-type starch is stronger than that in B-type starch.[32]

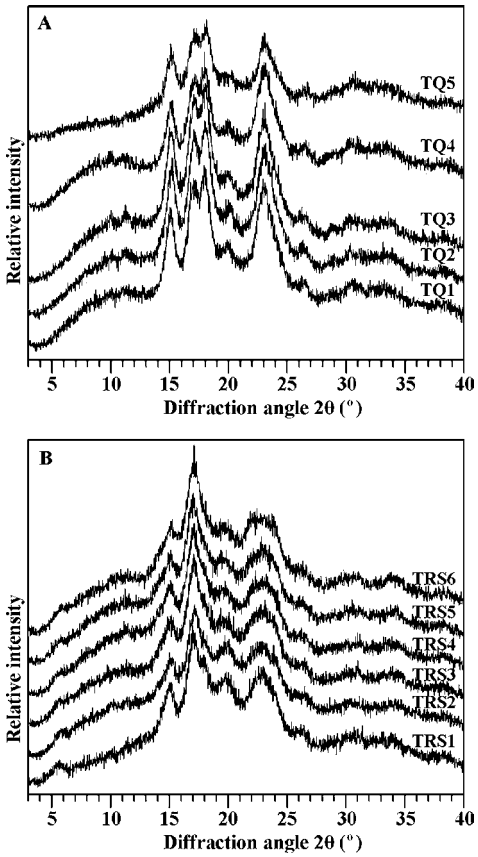

Figure 1. XRD spectra of in vitro digestive starch residues: (A) TQ starch residues; (B) TRS starch residues. TQ1, TQ2, TQ3, TQ4, and TQ5, TQ starch residues for 0, 1, 2, 4, and 8 h of digestion, respectively; TRS1, TRS2, TRS3, TRS4, TRS5, and TRS6, TRS starch residues for 0, 1, 2, 4, 8, and 16 h of digestion, respectively.

TQ control and in vitro digestive starch residues all displayed typical A-type XRD patterns. The peak intensities of starch residues for 1 and 2 h of digestion were similar to that of control starch. Upon 4 and 8 h of digestion, the peak intensities decreased in TQ starch (Figure 1A). TRS control starch showed a C_A-type XRD pattern with a shoulder peak at 18° 2θ (Figure 1B), which was in agreement with native TRS starch.[13] Although TRS control and in vitro digestive starch residues all showed similar XRD patterns, it was noteworthy that the intensity of the shoulder peak at 18° 2θ decreased, the peak at 23° 2θ became broader, and the peak at 15° 2θ became weaker with increasing digestion time. Two inconspicuous shoulder peaks at 22° and 24° 2θ appeared in starch residues for 16 h of digestion, which suggested that the starch residue was of C_B-type crystallinity (Figure 1B). The diffraction intensity variations of peaks at 15°, 18°, and 23° 2θ indicated that the ratio of B/A polymorph progressively increased during TRS starch in vitro digestion. That is to say, the A-type polymorph of TRS C-type starch was digested more quickly than the B-type polymorph. That the C-type starch became C_A- or C_B-type starch after enzyme hydrolysis has been reported.[33] In this study, in vitro digestion did not change the A-type crystallinity of TQ starch, but changed C_A-type crystallinity of TRS starch to C_B-type via C-type, which indicated that A-type crystallinity was susceptible to digestion and B-type crystallinity was resistant to digestion.

The relative crystallinities of TQ and TRS digestive starch residues were similar to those of TQ and TRS control starches, which indicated that both amorphous and crystalline structures of TQ and TRS starches were simultaneously hydrolyzed during in vitro digestion. Zhou et al.[34] also reported that both amorphous and semicrystalline regions of starch granules were simultaneously hydrolyzed by α-amylase, which was based on the observation that α-amylolysis did not produce a marked increase in the crystallinity.

^{13}C CP/MAS NMR Spectra of In Vitro Digestive Starch Residues. Figure 2A compares the ^{13}C CP/MAS NMR spectra of amorphous, control, and in vitro digestive TQ and TRS starch residues. TQ starch was rapidly digested, and there were not enough starch residues for ^{13}C CP/MAS NMR analysis after 4 h of in vitro digestion. Assignments of the ^{13}C CP/MAS NMR resonance are consistent with literature data.[35,36] Signals at 94−105 and 58−65 ppm are attributed to C1 and C6 in hexapyranoses, respectively; the overlapping signal around 68−78 ppm is associated with C2, C3, and C5,; and the broad resonance at 82 ppm appears from the amorphous domains for C4. The two broad shoulders that appear at 103 and 95 ppm can arise from the amorphous domains for C1. ^{13}C CP/MAS NMR has been employed in examining the structure of different type starches. In the spectra, most of the resonances cannot be distinguished or have not been assigned among the A-, B-, and C-type starches, but the C1 resonance contains information on the crystalline nature as well as the noncrystal-

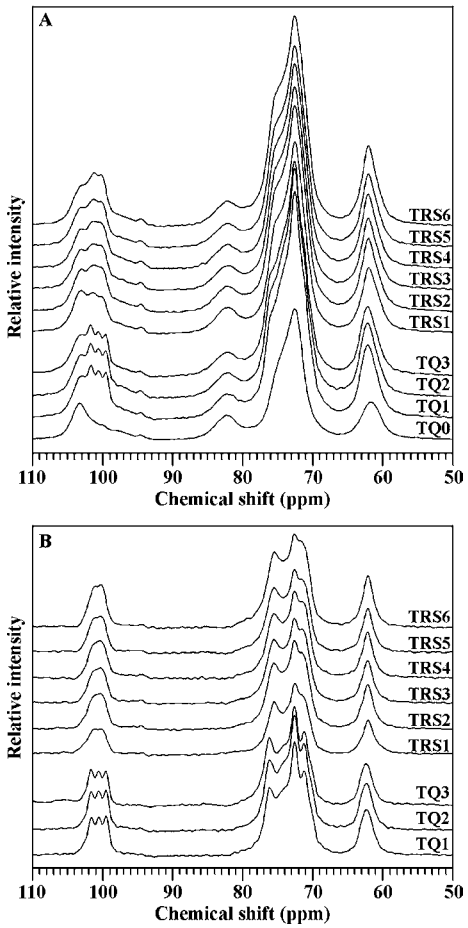

Figure 2. ^{13}C CP/MAS NMR spectra of in vitro digestive starch residues: (A) original spectra,; (B) ordered subspectra. TQ0, amorphous starch from TQ starch; TQ1, TQ2, and TQ3, TQ starch residues for 0, 1, and 2 h of digestion, respectively; TRS1, TRS2, TRS3, TRS4, TRS5, and TRS6, TRS starch residues for 0, 1, 2, 4, 8, and 16 h of digestion, respectively.

line (but rigid) chains. The multiplicity of the C1 resonance corresponds to the packing type of the starch granule. For A-type starch, the C1 peak of spectrum is a triplet, whereas for B-type starch, that is a doublet.[35] Because C-type starch has the characteristics of both A- and B-type crystalline structure, the C1 spectrum of the C-type starch always shows a mixed pattern of both A- and B-types. The resonances in the spectrum of C-type starch mainly depend on the relative proportions of A- or B-type crystallinity in the sample.[36] In general, the C-type starch shows a triplet C1 spectrum if the A-type crystalline structure is predominant in the sample and a doublet C1 spectrum if the B-type crystalline structure is predominant.[36]

The C1 resonances of TQ control starch occurred as triplets at about 99.5, 100.5, and 101.5 ppm, which was a typical characteristic of A-type starch.[36] The peak at about 103 ppm appeared only as a shoulder on the downfield C1 resonances in TQ control starch. These results were in agreement with that of native TQ starch.[13] The triplet and amorphous peaks of C1 resonances and their intensities in in vitro digestive TQ starch residues were very similar to that of TQ control starch, which suggested that digestion did not have an effect on molecular packing of the double helices in the crystalline regions, and both amorphous and crystalline components of starch were simultaneously hydrolyzed during in vitro digestion, which was in agreement with the results of XRD. The C1 resonances of TRS control starch occurred as inconspicuous triplets at 100.0, 100.8, and 101.4 ppm, and the peak at 103 ppm appeared as a strong peak, which was significantly different from that of TQ control starch and suggested that TRS control starch was a C_A-type starch. The ^{13}C CP/MAS NMR spectrum of TRS control starch was very similar to that of native TRS starch,[13] which was also in agreement with the results of XRD. The inconspicuous triplet gradually became a doublet at 100 and 101 ppm, which was the character of B-type starch, and the peak at 103 ppm became a shoulder peak with gradually decreasing peak intensity during in vitro digestion. The changes in the ^{13}C CP/MAS NMR patterns between TRS control and digestive starch residues revealed two important facts about the structural changes during in vitro digestion: (1) the amorphous starch was digested more rapidly than the crystalline starch; and (2) the A-type allomorph in the C-type starch was degraded more rapidly than the B-type polymorph.

Figure 2B is the ordered subspectra of control and in vitro digestive TQ and TRS starch residues, which involves the subtraction of a standard amorphous starch spectrum from the test spectrum until there is no residual intensity at 84 ppm (a region of the spectrum with intensity due solely to amorphous

Table 2. Relative Crystallinities and Proportions of Single-Helix, Double-Helix, and Amorphous Conformations Obtained from ^{13}C CP/MAS NMR Spectra of in Vitro Digestive Starch Residues[a]

			relative proportion[b] (%)		
	starch residue	relative crystallinity[c] (%)	single helix	double helix	amorphous
TQ					
	0 h	54.3 ± 2.5 ab	4.3 ± 1.0a	49.0 ± 1.0a	46.7 ± 1.1 a
	1 h	55.6 ± 1.2 a	2.0 ± 1.1 b	51.9 ± 1.1 b	46.1 ± 1.4 a
	2 h	47.2 ± 1.0 b	1.7 ± 0.2 b	49.8 ± 0.2 a	48.5 ± 0.9 a
TRS					
	0 h	38.4 ± 1.9 a	5.5 ± 0.8 a	39.9 ± 0.8 a	54.6 ± 0.9 a
	1 h	46.0 ± 2.8 b	2.6 ± 1.5 b	47.4 ± 1.5 b	50.0 ± 1.5 ab
	2 h	48.4 ± 1.9 b	2.7 ± 1.1 b	47.3 ± 1.1 b	50.0 ± 1.3 ab
	4 h	53.2 ± 1.3 c	2.0 ± 0.5 b	48.2 ± 0.5 b	49.8 ± 0.7 ab
	8 h	54.9 ± 1.7 c	2.2 ± 0.1 b	48.0 ± 0.0 b	49.8 ± 0.6 b
	16 h	54.1 ± 0.7 c	2.6 ± 0.6 b	49.8 ± 0.6 b	47.6 ± 0.8 b

[a]Data (mean ± SD) in the same column with different letters are significantly different ($p < 0.05$). [b]The relative proportion was calculated following the method of Tan et al.[27] [c]The relative crystallinity was calculated according to the method of Paris et al.[26]

conformations).[27] The ordered subspectra were similar to the origin spectra, but they had clearer crystalline peaks of C1 resonances than the origin spectra. The ordered subspectra with clear C1 triplets in TQ digestive starch residues were essentially similar to that in TQ control starch. The ordered subspectra in TRS digestive starch residues were different with that in TRS control starch. The C1 resonances gradually changed from inconspicuous triplets to a doublet, and its intensity gradually increased during in vitro digestion.

The ^{13}C CP/MAS NMR original spectra of in vitro digestive TQ and TRS starches were peak fitted by using peakfit; a combination (50/50) of Lorentzian and Gaussian profiles gave acceptable fitting ($r^2 > 0.99$) (data not shown). The percentage of relative crystallinity, which is quantitatively calculated as the proportion of the fitting peak areas of the triplet or doublet relative to the total area of the spectrum at C1 region according to the method described by Paris et al.,[26] is listed in Table 2. The crystallinity obtained from ^{13}C CP/MAS NMR was found to be higher than that from XRD for control and digestive starch residues. Molecular order in starch granule is composed of two types of helices from amylopectin side chains. Helices that are packed in regular arrays (in the long-range distance) forming crystallinity can be measured by both XRD and ^{13}C CP/MAS NMR. Helices that are not packed in regular form or packed in the short-range distance cannot be detected by XRD but can still be detected by ^{13}C CP/MAS NMR.[35] It is therefore not surprisingly that estimates of the relative crystallinities by ^{13}C CP/MAS NMR are considerably higher than those by XRD. The relative crystallinities obtained from XRD and ^{13}C CP/MAS NMR of TQ digestive starch residues were all similar to that of TQ control starch, which suggested that the long-range and short-range order structures and the amorphous structure were simultaneously hydrolyzed during TQ in vitro digestion. The relative crystallinities obtained from ^{13}C CP/MAS NMR of TRS digestive starch residues gradually increased with the digestion time elongation, but those obtained from XRD of TRS digestive starch residues were similar to those of TRS control, which suggested that the long-range order structure and amorphous structure were simultaneously hydrolyzed, and the short-range order structure was hydrolyzed more slowly than the amorphous structure during TRS in vitro digestion.

Additional information on the conformation of the starch polymers can be obtained by fitting of the ordered subspectra to individual peaks.[27] The ordered subspectra of control and in vitro digestive starch residues at the C1 region were peak fitted by using peakfit (data not shown). The results from quantitative analysis of the proportion of single helix, double helix, and amorphous components according to the method described by Tan et al.[27] are summarized in Table 2. The double helix and amorphous components of TQ digestive starch residues for 1 and 2 h of digestion were similar to those of TQ control starch, which was in agreement with the relative crystallinity obtained from XRD and ^{13}C CP/MAS NMR. The single helix was rapidly hydrolyzed in TQ in vitro digestion. This result further confirmed that the amorphous and crystalline components of TQ starch were simultaneously hydrolyzed by in vitro digestive enzymes. The amorphous and single helix was rapidly hydrolyzed, and the double helix proportion significantly increased in TRS starch as in vitro digestion took place. This result showed that the long-range and amorphous structures in TRS starch were hydrolyzed more quickly than the short-range order structure at the beginning of digestion. The double-helix proportion gradually increased in TRS digestive starch residues with digestion time elongation, which was in agreement with the relative crystallinity obtained from ^{13}C CP/MAS NMR and suggested that the short-range order structure was resistant to digestion.

ATR-FTIR Spectra of in Vitro Digestive Starch Residues. The development of sampling devices such as ATR-FTIR combined with procedures for spectrum deconvolution provides opportunities for the study of starch structure.[37] According to the theory of ATR, the penetration depth is related to the wavelength. Polysaccharides, such as starch, absorb in the region 1200−800 cm^{-1}, that is, at wavelengths between ∼8 and 12 μm. In this region, the average penetration depth is ∼2 μm. Therefore, ATR-FTIR is used to study the external region of the starch granule. According to van Soest et al.,[38] the infrared spectrum of starch has been shown to be sensitive to the short-range order structure, defined as the double-helical order, as opposed to the long-range order structure related to the packing of double helices. Although it has been proposed that FTIR is not related to XRD and is unable to differentiate starch long-range order characteristics and polymorphism, the spectrum variation of starch is interpreted in terms of the level of short-range order structure present on the edge of starch granules.[37] The absorbance band intensities at 1045, 1022, and 995 cm^{-1} are sensitive to changes in starch conformation. The bands at 1047 (or 1045) and 1022 cm^{-1} have been linked with order/crystallinity and amorphous regions in starch, respectively.[37] The ratio of absorbance 1045/1022 cm^{-1} is used to quantify the degree of order in starch samples. The intensity ratios of 1045/1022 and 1022/995 cm^{-1} are useful as a convenient index of FTIR data in comparisons with other measures of starch conformation.[39]

The deconvoluted ATR-FTIR spectra in the region 1200−900 cm^{-1} of control and in vitro digestive TQ and TRS starch residues are presented in Figure 3, panels A and B, respectively. The relative intensities of FTIR bands at 1045, 1022, and 995 cm^{-1} were recorded from the baseline to peak height, and the ratios for 1045/1022 and 1022/995 cm^{-1} were calculated as shown in Figure 3C. On the basis of both the spectra and calculated data, the short-range order in the external region of TQ in vitro digestive starch residues was similar to that of TQ control starch, which was in agreement with the relative crystallinity and double-helix proportion obtained from ^{13}C CP/MAS NMR. The short-range order in the external region of TRS in vitro digestive starch residues dramatically increased at the beginning of digestion and then gradually increased with digestion time elongation, which was also in agreement with the relative crystallinity and double-helix proportion obtained from ^{13}C CP/MAS NMR.

In Vivo Digestibilities of Starches. The enzymatic reactions in the in vitro digestion are carried out only in homogeneous solution/suspension, whereas the in vivo digestion takes place in the intestinal lumen and at the surface of the intestinal wall, both of which are likely to provide a heterogeneous environment. Furthermore, there are more enzymes involved in the intestinal digestion than in the in vitro digestion, for example, maltase-glucoamylase and sucrase-isomaltase versus fungal glucoamylase (also called amyloglucosidase), respectively. Therefore, the in vitro digestion might oversimplify the in vivo digestion mechanism. The results from in vitro starch digestion might not reflect that of in vivo starch digestion.[40] In this study, we used the diet containing 70% TQ or TRS flour to feed rat.[16] The in vivo digesta were collected

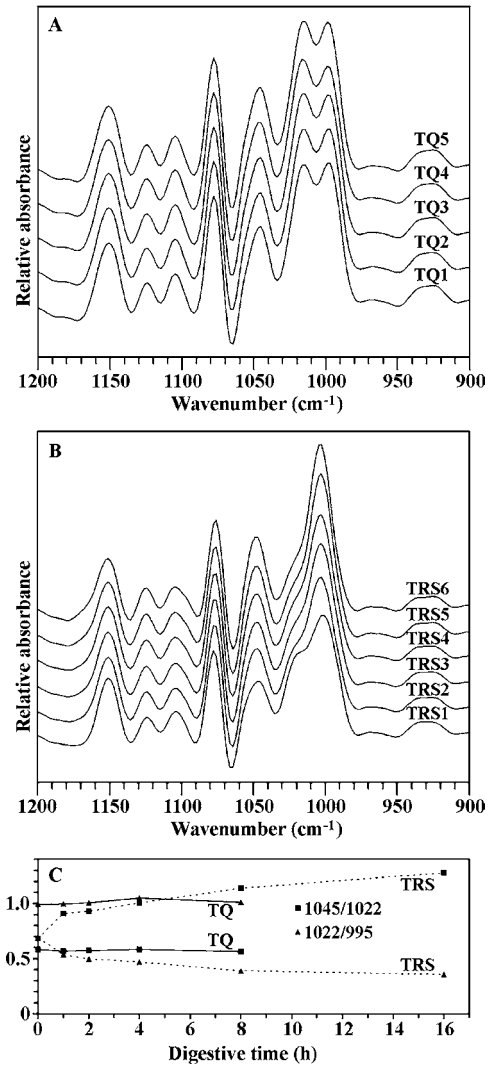

Figure 3. ATR-FTIR spectra of in vitro digestive starch residues: (A) TQ starch residues; (B) TRS starch residues; (C) IR ratio of absorbances 1045/1022 and 1022/995 cm^{-1}. TQ1, TQ2, TQ3, TQ4, and TQ5, TQ starch residues for 0, 1, 2, 4, and 8 h of digestion, respectively; TRS1, TRS2, TRS3, TRS4, TRS5, and TRS6, TRS starch residues for 0, 1, 2, 4, 8, and 16 h of digestion, respectively.

from the stomach, jejunum, and ileum of rats and observed using the light microscope. TRS starch residual granules could clearly be detected in the digesta of stomach, jejunum, and ileum of rat in TRS diet group. However, TQ starch residual granule was seldom detected in the digesta of ileum of rat in TQ diet group (data not shown). In the feces of rat in TRS diet group, TRS starch residual granule could randomly be observed; however, TQ starch residual granule could not be detected in the feces of rat in the TQ diet group (data not shown). The in vivo digestion indicated that TQ starch could be completely digested in the small intestine, but TRS starch could not be completely digested in the small intestine and could be degraded in the large intestine.

The in vivo digestive starch residues were isolated from the diet, digesta of stomach, jejunum, and ileum, and feces, and their structural changes were investigated using XRD, ^{13}C CP/MAS NMR, and ATR-FTIR. The quantity of starch residue from jejunum digesta of rats in the TQ diet group was too small to be investigated. The starch residues from feces did not show the spectrum patterns of XRD, ^{13}C CP/MAS NMR, and ATR-FTIR, so the data are not shown. Because the nonstarch material content was high in isolated starch residues, the amylose content and DSC thermal property were not analyzed, and the spectra of XRD, ^{13}C CP/MAS NMR, and ATR-FTIR were not quantitatively calculated for in vivo digestive starch residues.

XRD Spectra of in Vivo Digestive Starch Residues. The XRD spectra of in vivo digestive starch residues are shown in Figure 4. To exclude the effect of diet preparation on the

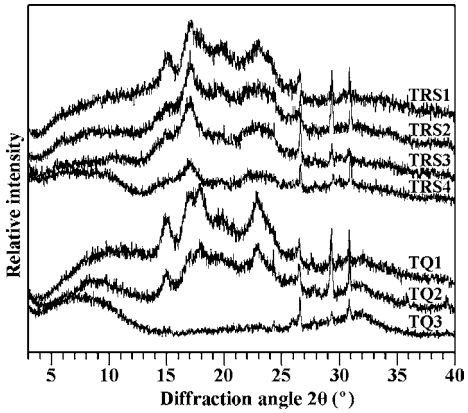

Figure 4. XRD spectra of in vivo digestive starch residues. TQ1, TQ2, and TQ3, TQ starch residues from diet and digesta of stomach and ileum of rat in TQ diet group, respectively; TRS1, TRS2, TRS3, and TRS4, TRS starch residues from diet and digesta of stomach, jejunum, and ileum of rat in TRS diet group, respectively.

structural properties of starch, the starches isolated from in vivo digesta were compared with those from diet. The starch isolated from the TQ diet showed the typical A-type XRD spectrum, which was similar to that of TQ in vitro control starch and suggested that the preparation process of the diet did not affect the crystallinity. The starch residues from stomach digesta of rats in the TQ diet group also showed A-type XRD spectra, although the peak intensity was significantly decreased. The starch residues from ileum digesta of rats in the TQ diet group did not show the starch XRD spectrum pattern, which might result from the low starch content in residues, and suggested that TQ starch was completely hydrolyzed in the small intestine.

The starch isolated from the TRS diet showed a C_A-type XRD spectrum with a shoulder peak of 18° 2θ, which was similar to that of TRS in vitro control starch. The starch residues from stomach, jejunum, and ileum digesta of rat in TRS diet group showed that the peak intensities gradually decreased, the shoulder peak at 18° 2θ disappeared, the peak at 23° 2θ became broader, and two inconspicuous shoulder peaks at 22° and 24° 2θ appeared during in vivo digestion. The spectrum changes of TRS in vivo digestive starch residues were in agreement with that of TRS in vitro digestive starch residues and indicated that the A-type polymorph of TRS C-type starch was digested more rapidly than the B-type polymorph. Although the peak intensity of starch residues from ileum digesta of rats in the TRS diet group was very low, the spectrum still showed the starch XRD pattern, which suggested that TRS starch was highly resistant to in vivo digestion.

^{13}C CP/MAS NMR Spectra of in Vivo Digestive Starch Residues. Figure 5 shows the original spectra and ordered subspectra of ^{13}C CP/MAS NMR of in vivo digestive starch.

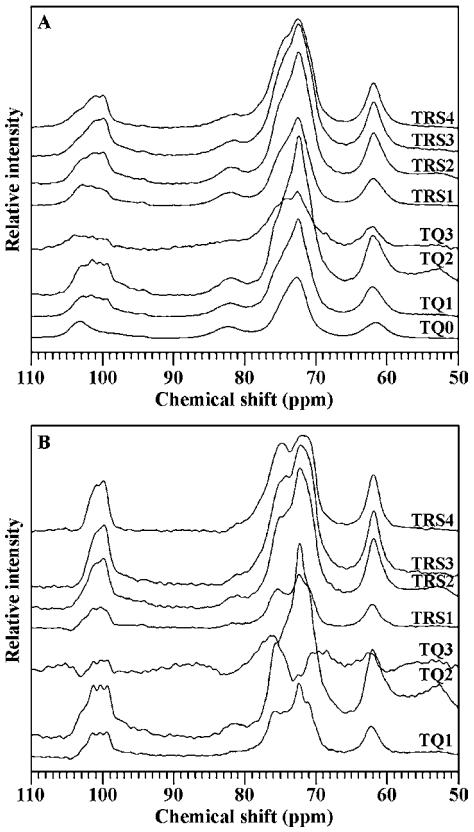

Figure 5. ^{13}C CP/MAS NMR spectra of in vivo digestive starch residues: (A) original spectra; (B) ordered subspectra. TQ0, amorphous starch from TQ starch; TQ1, TQ2, and TQ3, TQ starch residues from diet and digesta of stomach and ileum of rat in TQ diet group, respectively; TRS1, TRS2, TRS3, and TRS4, TRS starch residues from diet and digesta of stomach, jejunum, and ileum of rat in TRS diet group, respectively.

Compared with starch from the diet, the starch residues from stomach digesta of rats in the TQ diet group had higher crystallinity with triplets at C1 resonance, which was in agreement with that of TQ in vitro digestive starch. TQ starch residues from ileum digesta did not show the ^{13}C CP/MAS NMR spectrum pattern, which suggested that starch was essentially digested in the small intestine.

The ^{13}C CP/MAS NMR patterns between TRS diet and in vivo digestive starch residues revealed two important facts about the structural changes during in vivo digestion: (1) the amorphous starch was digested more rapidly than the crystalline starch; and (2) the A-type polymorph of TRS C-type starch was degraded more quickly than the B-type polymorph. The spectrum changes of TRS in vivo digestive starch residues were in agreement with those of TRS in vitro digestive starch residues. The TRS starch residues from ileum digesta still showed the typical ^{13}C CP/MAS NMR spectrum pattern; however, the TRS starch residues from feces did not show the ^{13}C CP/MAS NMR spectrum pattern (data not shown), which suggested that TRS starch was highly resistant to digestion in the small intestine and was degraded in the large intestine.

ATR-FTIR Spectra of in Vivo Digestion Starch Residues. The deconvoluted ATR-FTIR spectra in the region 1200−900 cm^{-1} of in vivo digestive starches are presented in Figure 6. The starch residues from the diet and stomach digesta of rats in the TQ diet group showed ATR-FTIR patterns

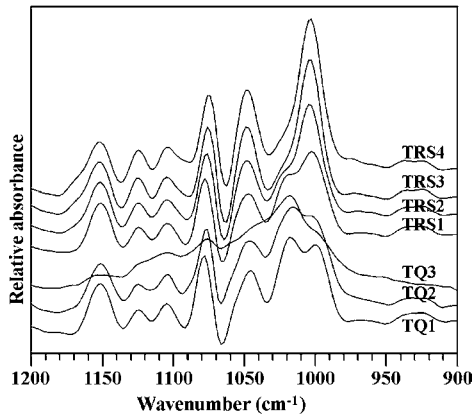

Figure 6. ATR-FTIR spectra of in vivo digestive starch residues. TQ1, TQ2, and TQ3, TQ starch residues from diet and digesta of stomach and ileum of rat in TQ diet group, respectively; TRS1, TRS2, TRS3, and TRS4, TRS starch residues from diet and digesta of stomach, jejunum, and ileum of rat in TRS diet group, respectively.

similar to that of TQ in vitro control and digestive starch residues. The starch residues from ileum digesta of rats in the TQ diet group did not show the starch ATR-FTIR spectrum pattern, which might result from the low starch content in residues, and suggested that TQ starch was susceptible to in vivo digestion. The starch residues from diet and digesta of stomach, jejunum, and ileum of rat in TRS diet group also showed similar ATR-FTIR patterns with TRS in vitro control and digestive starch residues. Starch residues from ileum digesta of rats in the TRS diet group showed the typical starch ATR-FTIR pattern, which suggested that TRS starch was highly resistant to in vivo digestion.

Although the ratios for 1045/1022 and 1022/995 cm^{-1} were not calculated, the spectra of starch residues clearly showed that the degree of the short-range order in the external region of TQ starch granule did not significantly change during in vivo digestion, but that of TRS starch significantly increased with in vivo digestion from stomach to jejunum and ileum. The ATR-FTIR spectrum changes of starch residues of in vivo digestion showed that the short-range order structure in the external region of TRS starch granule was highly resistant to digestion, which was in agreement with that of in vitro digestion.

In conclusion, starches were isolated from mature grains of high-amylose TRS and its wild-type rice TQ. The structural changes of starch residues following in vitro digestion were characterized with DSC, XRD, ^{13}C CP/MAS NMR, and ATR-FTIR. TQ control and digestive starch residues did not show significant structural changes, which suggested that both amorphous and crystalline structures were simultaneously hydrolyzed during in vitro digestion. The A-type polymorph of TRS C-type starch was hydrolyzed more quickly than the B-type polymorph. Although both amorphous and crystalline (long-range order) structures were simultaneously digested in TRS starch, the short-range order (double-helix) structure, especially in the external region of starch granule, was highly resistant to digestion. Furthermore, the structural changes of starch residues following in vivo digestion were in agreement with those of in vitro digestion. These data added to our understanding of the resistance of high-amylose rice starch to digestion and would be very helpful in the application of high-amylose rice TRS in food and nonfood industries.

dx.doi.org/10.1021/jf302966f | J. Agric. Food Chem. 2012, 60, 9332−9341

AUTHOR INFORMATION

Corresponding Author

*(Q.L.) Postal address: Agricultural College, Yangzhou University, Yangzhou 225009, China. Phone: +86 514 87996648. E-mail: qqliu@yzu.edu.cn. (C.W.) Postal address: College of Bioscience and Biotechnology, Yangzhou University, Yangzhou 225009, China. Phone: +86 514 87997217. E-mail: cxwei@yzu.edu.cn.

Funding

This study was financially supported by grants from the Ministry of Science and Technology of China (2012CB944803), the National Natural Science Foundation of China (31071342, 31270221), and the Funds for Distinguished Young Scientists (BK201210) and Priority Academic Program Development from Jiangsu Government, China.

Notes

The authors declare no competing financial interest.

ABBREVIATIONS USED

ATR-FTIR, attenuated total reflectance−Fourier transform infrared; ^{13}C CP/MAS NMR, ^{13}C cross-polarization magic-angle spinning nuclear magnetic resonance; DSC, differential scanning calorimetry; SBE, starch branching enzyme; RS, resistant starch; TQ, Te-qing (wild-type rice cultivar); TRS, transgenic rice line; XRD, X-ray powder diffraction.

REFERENCES

(1) Englyst, H. N.; Kingman, S. M.; Cummings, J. H. Classification and measurement of nutritionally important starch fractions. *Eur. J. Clin. Nutr.* **1992**, *46*, S33−S50.

(2) Nugent, A. P. Health properties of resistant starch. *Nutr. Bull.* **2005**, *30*, 27−54.

(3) Sang, Y. J.; Bean, S.; Seib, P. A.; Pedersen, J.; Shi, Y. C. Structure and functional properties of sorghum starches differing in amylose content. *J. Agric. Food Chem.* **2008**, *56*, 6680−6685.

(4) Butardo, V. M.; Fitzgerald, M. A.; Bird, A. R.; Gidley, M. J.; Flanagan, B. M.; Larroque, O.; Resurreccion, A. P.; Laidlaw, H. K. C.; Jobling, S. A.; Morell, M. K.; Rahman, S. Impact of down-regulation of *starch branching enzyme IIb* in rice by artificial microRNA- and hairpin RNA-mediated RNA silencing. *J. Exp. Bot.* **2011**, *62*, 4927−4941.

(5) Garwood, D. L.; Shannon, J. C.; Creech, R. G. Starches of endosperms possessing different alleles at the *amylose-extender* locus in *Zea mays* L. *Cereal Chem.* **1976**, *53*, 355−364.

(6) Regina, A.; Bird, A.; Topping, D.; Bowden, S.; Freeman, J.; Barsby, T.; Kosar-Hashemi, B.; Li, Z. Y.; Rahman, S.; Morell, M. High-amylose wheat generated by RNA interference improves indices of large-bowel health in rats. *Proc. Natl. Acad. Sci. U.S.A.* **2006**, *103*, 3546−3551.

(7) Regina, A.; Kosar-Hashemi, B.; Ling, S.; Li, Z. Y.; Rahman, S.; Morell, M. Control of starch branching in barley defined through differential RNAi suppression of starch branching enzyme IIa and IIb. *J. Exp. Bot.* **2010**, *61*, 1469−1482.

(8) Satoh, H.; Nishi, A.; Yamashita, K.; Takemoto, Y.; Tanaka, Y.; Hosaka, Y.; Sakurai, A.; Fujita, N.; Nakamura, Y. Starch-branching enzyme I-deficient mutation specifically affects the structure and properties of starch in rice endosperm. *Plant Physiol.* **2003**, *133*, 1111−1121.

(9) Mizuno, K.; Kawasaki, T.; Shimada, H.; Satoh, H.; Kobayashi, E.; Okumura, S.; Arai, Y.; Baba, T. Alteration of the structural properties of starch components by the lack of an isoform of starch branching enzyme in rice seeds. *J. Biol. Chem.* **1993**, *268*, 19084−19091.

(10) Bird, A. R.; Jackson, M.; King, R. A.; Davies, D. A.; Usher, S.; Topping, D. L. A novel high-amylose barley cultivar (*Hordeum vulgare* var. *Himalaya 292*) lowers plasma cholesterol and alters indices of large-bowel fermentation in pigs. *Br. J. Nutr.* **2004**, *92*, 607−615.

(11) Kang, H. J.; Hwang, I. K.; Kim, K. S.; Choi, H. C. Comparative structure and physicochemical properties of IIpumbyeo, a high-quality japonica rice, and its mutant, Suweon 464. *J. Agric. Food Chem.* **2003**, *51*, 6598−6603.

(12) Yano, M.; Okuno, K.; Kawakami, J.; Satoh, H.; Omura, T. High amylose mutants of rice, *Oryza sativa* L. *Theor. Appl. Genet.* **1985**, *69*, 253−257.

(13) Wei, C. X.; Xu, B.; Qin, F. L.; Yu, H. G.; Chen, C.; Meng, X. L.; Zhu, L. J.; Wang, Y. P.; Gu, M. H.; Liu, Q. Q. C-type starch from high-amylose rice resistant starch granules modified by antisense RNA inhibition of starch branching enzyme. *J. Agric. Food Chem.* **2010**, *58*, 7383−7388.

(14) Zhu, L. J.; Gu, M. H.; Meng, X. L.; Cheung, S. C. K.; Yu, H. X.; Huang, J.; Sun, Y.; Shi, Y. C.; Liu, Q. Q. High-amylose rice improves indices of animal health in normal and diabetic rats. *Plant Biotechnol. J.* **2012**, *10*, 353−362.

(15) Wei, C. X.; Qin, F. L.; Zhou, W. D.; Xu, B.; Chen, C.; Chen, Y. F.; Wang, Y. P.; Gu, M. H.; Liu, Q. Q. Comparison of the crystalline properties and structural changes of starches from high-amylose transgenic rice and its wild type during heating. *Food Chem.* **2011**, *128*, 645−652.

(16) Zhou, X. H.; Dong, Y.; Xiao, X.; Wang, Y.; Xu, Y.; Xu, B.; Shi, W. D.; Zhang, Y.; Zhu, L. J.; Liu, Q. Q. A 90-day toxicology study of high-amylose transgenic rice grain in Sprague-Dawley rats. *Food Chem. Toxicol.* **2011**, *49*, 3112−3118.

(17) Gray, G. M. Starch digestion and absorption in nonruminants. *J. Nutr.* **1992**, *122*, 172−177.

(18) Botham, R. L.; Cairns, P.; Morris, V. J.; Ring, S. G.; Englyst, H. N.; Cummings, J. H. A physicochemical characterization of chick pea starch resistant to digestion in the human small intestine. *Carbohydr. Polym.* **1995**, *26*, 85−90.

(19) Englyst, H. N.; Kingman, S. M.; Hudson, G. J.; Cummings, J. H. Measurement of resistant starch in vitro and in vivo. *Br. J. Nutr.* **1996**, *75*, 749−755.

(20) Zhang, G.; Ao, Z.; Hamaker, B. R. Nutritional property of endosperm starches from maize mutants: a parabolic relationship between slowly digestible starch and amylopectin fine structure. *J. Agric. Food Chem.* **2008**, *56*, 4686−4694.

(21) Witt, T.; Gidley, M. J.; Gilbert, R. G. Starch digestion mechanistic information from the time evolution of molecular size distributions. *J. Agric. Food Chem.* **2010**, *58*, 8444−8452.

(22) McCleary, B. V.; McNally, M.; Rossiter, P. Measurement of resistant starch by enzymatic digestion in starch and selected plant materials: collaborative study. *J. AOAC Int.* **2002**, *85*, 1103−1111.

(23) Wei, C. X.; Qin, F. L.; Zhu, L. J.; Zhou, W. D.; Chen, Y. F.; Wang, Y. P.; Gu, M. H.; Liu, Q. Q. Microstructure and ultrastructure of high-amylose rice resistant starch granules modified by antisense RNA inhibition of starch branching enzyme. *J. Agric. Food Chem.* **2010**, *58*, 1224−1232.

(24) Konik-Rose, C.; Thistleton, J.; Chanvrier, H.; Tan, I.; Halley, P.; Gidley, M.; Kosar-Hashemi, B.; Wang, H.; Larroque, O.; Ikea, J.; McMaugh, S.; Regina, A.; Rahman, S.; Morell, M.; Li, Z. Effects of starch synthase IIa gene dosage on grain, protein and starch in endosperm of wheat. *Theor. Appl. Genet.* **2007**, *115*, 1053−1065.

(25) Wei, C. X.; Qin, F. L.; Zhou, W. D.; Yu, H. G.; Xu, B.; Chen, C.; Zhu, L. J.; Wang, Y. P.; Gu, M. H.; Liu, Q. Q. Granule structure and distribution of allomorphs in C-type high-amylose rice starch granule modified by antisense RNA inhibition of starch branching enzyme. *J. Agric. Food Chem.* **2010**, *58*, 11946−11954.

(26) Paris, M.; Bizot, H.; Emery, J.; Buzaré, J. Y.; Buléon, A. Crystallinity and structuring role of water in native and recrystallized starches by ^{13}C CP-MAS NMR spectroscopy 1: spectral decomposition. *Carbohydr. Polym.* **1999**, *39*, 327−339.

(27) Tan, I.; Flanagan, B. M.; Halley, P. J.; Whittaker, A. K.; Gidley, M. J. A method for estimating the nature and relative proportions of amorphous, single, and double-helical components in starch granules by ^{13}C CP/MAS NMR. *Biomacromolecules* **2007**, *8*, 885−891.

(28) Zhu, L. J.; Liu, Q. Q.; Wilson, J. D.; Gu, M. H.; Shi, Y. C. Digestibility and physicochemical properties of rice (*Oryza sativa* L.) flours and starches differing in amylose content. *Carbohydr. Polym.* **2011**, *86*, 1751−1759.
(29) Gérard, C.; Colonna, P.; Buléon, A.; Planchot, V. Amylolysis of maize mutant starches. *J. Sci. Food Agric.* **2001**, *81*, 1281−1287.
(30) Miao, M.; Zhang, T.; Mu, W. M.; Jiang, B. Structural characterizations of waxy maize starch residue following in vitro pancreatin and amyloglucosidase synergistic hydrolysis. *Food Hydrocolloids* **2011**, *25*, 214−220.
(31) Cooke, D.; Gidley, M. J. Loss of crystalline and molecular order during starch gelatinisation: origin of the enthalpic transition. *Carbohydr. Res.* **1992**, *227*, 103−112.
(32) Cheetham, N. W. H.; Tao, L. Variation in crystalline type with amylose content in maize starch granules: an X-ray powder diffraction study. *Carbohydr. Polym.* **1998**, *36*, 277−284.
(33) Jiang, Q. Q.; Gao, W. Y.; Li, X.; Zhang, J. Z. Characteristics of native and enzymatically hydrolyzed *Zea mays* L., *Fritillaria ussuriensis* Maxim. and *Dioscorea opposita* Thunb. starches. *Food Hydrocolloids* **2011**, *25*, 521−528.
(34) Zhou, Y.; Hoover, R.; Liu, Q. Relationship between α-amylase degradation and the structure and physicochemical properties of legume starches. *Carbohydr. Polym.* **2004**, *57*, 299−317.
(35) Atichokudomchai, N.; Varavinit, S.; Chinachoti, P. A study of ordered structure in acid-modified tapioca starch by ^{13}C CP/MAS solid-state NMR. *Carbohydr. Polym.* **2004**, *58*, 383−389.
(36) Bogracheva, T. Y.; Wang, Y. L.; Hedley, C. L. The effect of water content on the ordered/disordered structures in starches. *Biopolymers* **2001**, *58*, 247−259.
(37) Sevenou, O.; Hill, S. E.; Farhat, I. A.; Mitchell, J. R. Organisation of the external region of the starch granule as determined by infrared spectroscopy. *Int. J. Biol. Macromol.* **2002**, *31*, 79−85.
(38) van Soest, J. J. G.; Tournois, H.; de Wit, D.; Vliegenthart, J. F. G. Short-range structure in (partially) crystalline potato starch determined with attenuated total reflectance Fourier-transform IR spectroscopy. *Carbohydr. Res.* **1995**, *279*, 201−214.
(39) Htoon, A.; Shrestha, A. K.; Flanagan, B. M.; Lopez-Rubio, A.; Bird, A. R.; Gilbert, E. P.; Gidley, M. J. Effects of processing high amylose maize starches under controlled conditions on structural organisation and amylase digestibility. *Carbohydr. Polym.* **2009**, *75*, 236−245.
(40) Hasjim, J.; Lavau, G. C.; Gidley, M. J.; Gilbert, R. G. In vivo and in vitro starch digestion: are current in vitro techniques adequate. *Biomacromolecules* **2011**, *11*, 3600−3608.